Cooperativity at the glass transition: A perspective from facilitation on the analysis of relaxation in modulated calorimetry

Elpidio Tombari
CNR, Istituto per i Processi Chimico-Fisici, v. Moruzzi 1, 56124 Pisa, Italy

Marco Pieruccini
CNR, Istituto Nanoscienze, v. Campi 213/A, 41125 Modena, Italy

(Received 29 January 2016; revised manuscript received 6 October 2016; published 28 November 2016)

The glass transition region in nonconfined polymeric and low-molecular-weight supercooled liquids is probed by temperature-modulated calorimetry at a frequency of 3.3 mHz. From the distribution of relaxation times derived by analyzing the complex heat capacity, the number N_α of cooperatively rearranging units is estimated. This is done by resorting to a method in which cooperative motion is viewed as a result of a spontaneous regression of energy fluctuations. After a first, local, structural transition occurs, the energy threshold for the rearrangement of adjacent molecular units decreases progressively. This facilitation process is associated to a corresponding evolution of the density of states in a canonical representation and may be considered as a continuous spanning through different dynamic states toward a condition in which configurational constraints disappear. A good agreement is found with the N_α values obtained from the same calorimetric data within the framework of Donth's fluctuation theory. It is shown that, at variance from previous treatments, N_α can be estimated from just the relaxation function, without resorting to the knowledge of the configurational entropy. Examples point to a modest dependence of the N_α estimates on the experimental method used to derive the relaxation function.

DOI: 10.1103/PhysRevE.94.052504

I. INTRODUCTION

The super-arrhenian behavior characterizing the viscosity of liquids approaching the glass transition temperature inspired the idea that, upon cooling, structural rearrangements (the so-called α-process) would take place cooperatively within domains of progressively increasing size. Together with the general interest for the understanding of the glass transition process itself, such an hypothesis motivated the efforts devoted to the experimental determination of the extension of these domains.

At present such measurements cannot be done directly; instead, models were developed with the aim of finding support to this concept through a coherent analysis of calorimetric or relaxation data. In this sense, recent literature provided evidences of a growing cooperativity length scale on cooling, the significance of these results resting also upon the mutual consistency of the conclusions drawn from seemingly different data analyses. Donth's fluctuation theory [1,2] has been applied to calorimetric or dielectric relaxation data, e.g., in Refs. [3,4], while a four-point correlation function approach [5] was considered in Refs. [6,7]. A thorough comparison between Donth's and four-point based estimates of the number of units (e.g., monomers in the case of polymers) forming the cooperatively rearranging regions (CRRs), has been also provided by Rijal *et al.* for a number of systems [8].

Besides the above-mentioned methods a further one has been proposed, in which the structural relaxation is viewed as an effect of a spontaneous regression of energy fluctuations [9,10]. A central point in this description is that the structural change in a CRR initiates from the rearrangement of a few units; then, after this *small scale* process has started, part of the energy initially gained by these units flows into the configurational degrees of freedom of the surrounding region during the fluctuation regression, this way inducing a cooperative configurational change over a larger domain (the whole CRR indeed).

More explicitly, based on a statistical mechanical description of the small-scale process, a relaxation function was derived [Eq. (7) below] in order to fit the data and extract relevant parameters, such as the number z of units initiating the structural change and the average energy threshold these units had to overcome for a rearrangement [11]. The size of the region where the subsequent *large scale* rearrangement takes place was then estimated via the specific configurational entropy, s_c, known from the experiment [Eq. (12) below] [9,10].

Of course, a crucial hypothesis in that method is that the energy transfer between the small-scale region and the configurational degrees of freedom of the large-scale domain be efficient. For this reason, polymers were considered for a first test of the model and, indeed, the agreement with the literature results obtained in the light of Donth's theory was satisfactory [10].

There are, however, at least two points deserving further consideration. The first, which may appear rather technical, relates to the fact that, irrespective of the spectroscopic technique that is used to get the relaxation function, the CRR size could not be calculated without knowing s_c. On the other hand, the possibility to perform such estimates without the need to rely upon calorimetric data anyway would be advantageous, also because all issues relating to interpretations of the actual form of s_c would be bypassed.

The other point has to do with the possibility of extending the application of the method to low-molecular-weight systems. In this case, chain connectivity is lacking and the mechanism of energy transfer from small- to large-scale domains, envisaged in the former version of the theory, cannot be expected to hold anymore. An alternative picture could be that large-scale diffusional motion may result from a progressive

weakening of the configurational constraints, triggered by the initial small-scale rearrangement in a sort of avalanche process. This reductive pictorial description nevertheless represents the rather nontrivial concept of facilitation, which is actually given quite a role in recent studies on the glass transition [12,13].

It is the aim of this paper to provide a unique thermodynamic, semiphenomenological description for large-scale modes excitation suited for both polymeric and low-molecular-weight liquids. This will be done in a form consistent with the idea of facilitation. It will be also shown that all information relevant to the determination of the cooperativity in nonconfined systems, at least in proximity of the glass transition, is already present in the relaxation function itself, thus relieving s_c from the central role it had before.

The analysis of experimental data is of course not only the final practical motivation for the development of our arguments but also a way for assessing their significance. In this respect, reference to Donth's fluctuation approach is particularly important because the present treatment focuses on fluctuations as well. For this reason we derive the number N_α of cooperatively rearranging units (shortly cooperativity) with both Donth's method and the present one from the *same* set of data, namely from the heat capacity of polymeric and low molecular weight liquids probed at a very low frequency around their glass transition temperature. One may object that it wouldn't be worth making an effort to avoid the use of calorimetric data for the calculation of s_c, if at the end of the story the relaxation function is derived from the complex heat capacity itself. The aspect we wish to point out here, though, is that the cooperativity can be estimated from the analysis of the relaxation function only, be it obtained from dielectric, mechanical, NMR [9,10,14–17], or other kinds of experimental techniques.

II. THEORY

In analogy with the picture given by Adam and Gibbs [18], a configurational transition in the whole CRR may take place after an energy fluctuation overcomes a certain threshold. In our scheme this threshold is not unique: it does have a nonzero mean indeed (see below), but it otherwise depends on the local constraints characterizing the small-scale region where a rearrangement happens to initiate. Since these constraints are related to the actual configuration, the rearrangement barrier of any small scale domain changes with time as well. The characteristic lifetime of a structural state whatsoever is thus distributed and changes during the relaxation process. Below, when experimental data will be analyzed, we shall assume that the observed spectrum is in fact determined by the lifetime distribution of the structural states.

Following the general theory of thermodynamic fluctuations [19], we consider the CRRs as subsystems maintaining an internal equilibrium even during (small) deviations from equilibrium with respect to the environment; internal fluctuations are of course allowed.

Within a CRR there are units with an associated energy ϵ larger than the local threshold ζ established by the actual constraints (a well of depth ζ, in fact) and units for which this is not the case; the former are in a condition of mobility while the others are considered in a frozen metastable state with respect to the diffusional motion. Figure 1 shows schematically this distinction, together with some of the paths allowing for local rearrangements. Trajectories labeled with an "a" are always permitted, while those labeled with "b" are prohibited unless the well depth ζ changes as an effect of local rearrangements taking place in the close surroundings. In the latter case, the occurrence of a decrease in the threshold height corresponds to facilitation.

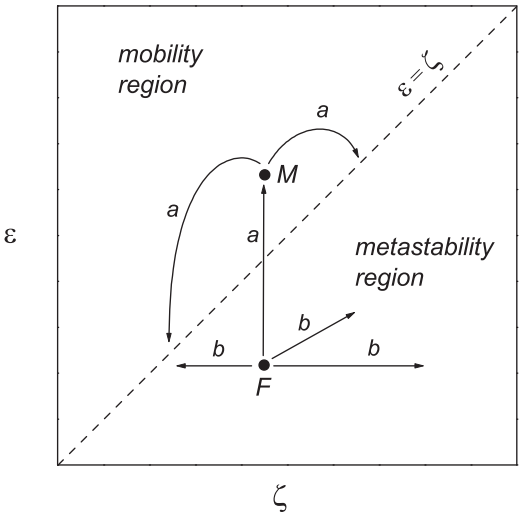

FIG. 1. Mobility and metastability regions to which a unit with energy ϵ may belong when the rearrangement threshold energy is ζ. If the latter is fixed, that is, when no rearrangement occurring in the surroundings of the unit is able to change it, a state characterized by a different threshold can only be reached after a passage through the mobility region; so, the paths labeled with an "a" are allowed while the others are not. After a unit has left its frozen state "F" to reach the mobility state "M" with an energy fluctuation, the subsequent value of the rearrangement threshold is random.

The ensemble of CRRs is distributed around averages with respect to both size and deviation from the minimum value of the free energy. Deferring to future work a more detailed treatment, we shall consider for simplicity a CRR ensemble in which all the elements are characterized by the same size and deviation from equilibrium (eventually, the model will be used to fit experimental data and the size and free energy ascribed to a CRR will be considered as the averages characterizing the ensemble at the temperature at which the measurements were done). Internal CRR fluctuations may cause local rearrangements triggering the large-scale configurational changes and will not be neglected; they describe a complex dynamics whereby the mobile units restlessly change their local environment, probing in the course of time different values of the energy threshold ζ. In steady conditions the ensemble of mobile units is described by a stationary distribution that extremizes a suitable thermodynamic potential explicitly derived below.

We start with assigning a partition function to a single unit in the mobility state:

$$Z_{\zeta,n} \equiv \int_\zeta^\infty d\epsilon\, \epsilon^n\, e^{-\epsilon/k_BT} = (k_BT)^{n+1}\Gamma(n+1,\zeta/k_BT), \quad (1)$$

with $k_B T$ the thermal energy and n an integer parametrizing the density of states. The integrand in $Z_{\zeta,n}$ is the same one would find for an ensemble of $n+1$ thermalized independent oscillators. This assumption is suggested by the results of neutron scattering experiments that, for liquids in physical conditions similar to those considered here, indicate in a wandering about fixed sites the main character of the units' motion, a change of mean position taking place only occasionally [20,21]. From the above partition function, the excess chemical potential with respect to the equilibrium state can be readily given in terms of the probability $w(\zeta,n) \equiv Z_{\zeta,n}/Z_{0,n}$:

$$\Delta\mu(\zeta,n) \equiv -k_B T \ln w. \tag{2}$$

This quantity is involved in the condition that the CRR ensemble be characterized by a fixed deviation from equilibrium [cf. Eq. (5) below].

For the construction of our thermodynamic potential we have to take into account that the ζ value of a unit undergoes random changes. The occurrence of nearby local readjustments is a possible cause of this randomization; however, as illustrated above, re-entering from the mobility region into a metastable state is assumed to be a relevant mechanism too in this sense, and indeed, the really important one in local rearrangements or at the beginning of large-scale structural transitions (cf. Fig. 1), when facilitation is not yet active. This loss of information is expressed through the entropy associated to the distribution of mobile units, $p(\zeta,n)$, characterizing the stationary state of the CRR ensemble:

$$S = -k_B \int_0^{+\infty} d\zeta \; p(\zeta,n) \ln p(\zeta,n). \tag{3}$$

On the other hand, taking the average energy of a unit in the form $w\langle E\rangle_{\zeta,n}$, with

$$\langle E\rangle_{\zeta,n} \equiv Z_{\zeta,n+1}/Z_{\zeta,n} \tag{4}$$

(i.e., a mean calculated over energy levels $\epsilon \geqslant \zeta$), we arrive at the "constrained" potential,

$$A[p] \equiv U - TS + \lambda\overline{\Delta\mu}\,, \tag{5}$$

where $U = \int_0^{+\infty} d\zeta \; p\langle E\rangle_{\zeta,n} w$ and $\overline{\Delta\mu} = \int_0^{+\infty} d\zeta \; p\,\Delta\mu$; λ, instead, is the Lagrange multiplier associated to the condition that the deviation from equilibrium of the CRR ensemble is fixed [11]. Extremizing A with respect to p one finds the distribution of a thermalized population of mobile units; a straightforward procedure yields

$$p(\zeta,n) \sim w^{\lambda}\, e^{-w\langle E\rangle_{\zeta,n}/k_B T}. \tag{6}$$

The factor w^{λ} in Eq. (6) indicates that a unit may reach the mobility region (by absorbing on average the energy $w\langle E\rangle_{\zeta,n}$) provided λ more units in close vicinity occupy, each of them, energy levels $\epsilon \geqslant \zeta$. These units do not need be actually rearranging; one can imagine, for instance, that they participate to a sort of collective oscillatory motion precursory to, or supporting, the small-scale readjustment. As shown explicitly with Eq. (15) below, the term w^{λ} describes a "free energy" cost to be paid for a unit to reach mobility and possibly rearrange. An analogous circumstance is found in first-order phase transitions, where a positive free energy necessarily sets in at the surface of the nuclei of a stable phase, forming in the parent metastable phase. In the present case, the specific value of this free energy is $\Delta\mu(\zeta,n)$. The dynamic regime of the units supporting local rearrangement contributes to what will be called "dynamic interfacial free energy" throughout. We want to recommend not to associate it to the ordinary geometrical idea of a surface separating two substances or two phases of the same material. Here indeed, this interface is meant as a dynamic condition separating in a certain sense a state of frozen configurational degrees of freedom from a state where no such constraints exist at all.

Once the distribution $p(\zeta,n)$ is obtained, the relaxation function can be expressed as a superposition of single-time contributions [11]:

$$\phi(t) \sim \int_0^{\infty} d\zeta \; p(\zeta,n) \exp\{-t\, \nu^* e^{-z\,\Delta\mu(\zeta,n)/k_B T}\}, \tag{7}$$

where t is the time, ν^* is a characteristic attempt rate, and z is the average number of units initiating the rearrangement.

Data analysis consists in fitting the experimental relaxation function associated to the α process with the above one; this yields λ, n, z and ν^*. Past work carried out on a variety of systems in different conditions (see Ref. [10] and literature cited therein) point out that the average energy barrier $\langle\zeta\rangle$ increases on cooling; furthermore, the actual fitting values of λ are

(1) often larger than the corresponding values found for z (or equal just by chance),

(2) monotonically increasing with n (and usually close to it),

(3) increasing on cooling.

These points indicate that z and λ refer to distinct objects and suggest that, in fact, $z\lambda$ units support a dynamic interface (with respect to the dynamic state of the almost frozen rest of the system) for the z units initiating the rearrangement. The above items also indicate that, upon cooling, the formation of critical mobile nuclei require crossing progressively higher free energy barriers [e.g., data analysis hints at a growth in $\lambda\,\overline{\Delta\mu}$]. An increase of λ (and thus n) on lowering T indicates that the density of high-energy states grows upon cooling; this mechanism enhances the efficiency to gain energy by fluctuation, because the number of available states gets larger (similar arguments can be found in Ref. [22]). So, the possibility of local small-scale transitions for the z units requires that a sufficient (dynamic) interfacial free energy is established in advance. Finally, the above listed observations also point to the relation $\partial\lambda/\partial\langle\zeta\rangle > 0$, linking average barrier height $\langle\zeta\rangle$ and number λ of supporting units *at the beginning* of a structural transition.

Within a regime of constant n, that is, before a large-scale structural transition initiates at a given T, the presence of the dynamic interface allows z units to explore the space of all available threshold values without undergoing significant diffusive motion, thus keeping in a restricted spatial region (path "a" in Fig. 2). A transition to a new "dynamic phase" where large-scale configurational motion sets in, would require that the density of states increases at low energies and decreases at high energies. This is because in a regime where diffusional motion dominates, the occurrence of high-energy barriers is rare. A suitable decrease in n describes this dynamic change (cf. the inset of Fig. 2). On the other hand [10], the

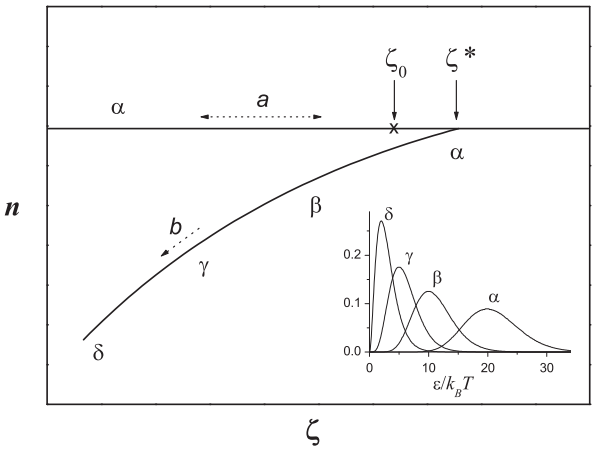

FIG. 2. Along the $n = \text{const.}$ line (labeled with a), the z units span the available ζ domain while remaining in the small-scale rearrangement regime. A dynamic transition may only start for ζ larger than ζ_0, that is, the threshold value for which the equality holds in Eq. (8) of the text; ζ^* is one such value at which the transition toward a large scale rearrangement happens to start, with the representative point of the local rearranging set of units following the downward curved $\Delta\mu(n,\zeta) = \text{const.}$ line (labeled with b). The curves of the inset represent examples of the normalized integrand of the partition function $Z_{\zeta,n}$ for different values of n, namely 20, 10, 5, and 2, which are labeled as α, β, γ, and δ, respectively. The labels on lines a and b highlight a correspondence of different dynamic regimes with the probability profiles of the inset.

transition from a confined to a diffusive dynamics may take place spontaneously for all ζ's, such that

$$\Delta\mu(\zeta,n) \gtrsim T s_c \tag{8}$$

(whatever the value or form of the entropy s_c), i.e., when the probability associated to a final configurational state, e^{-s_c/k_B}, is larger than the probability $Z_{\zeta,n}/Z_{0,n}$ for a unit to be in a high-energy state. This condition is fulfilled whenever $\zeta \geqslant \zeta_{0,n}$, where $\zeta_{0,n}$ is the solution of Eq. (8) set as an equality.

One may wonder whether it is possible that n decreases while maintaining the inequality of Eq. (8). In fact, from the definitions of Eqs. (1) and (2) it follows that

$$\begin{array}{ll} \left(\frac{\partial\Delta\mu}{\partial n}\right)_{T,\zeta} & < 0 \\ \left(\frac{\partial\Delta\mu}{\partial \zeta}\right)_{T,n} & > 0 \\ \left.\frac{d\zeta}{dn}\right|_{\Delta\mu} & \equiv -\left(\frac{\partial\Delta\mu}{\partial\zeta}\right)_T^{-1}\left(\frac{\partial\Delta\mu}{\partial n}\right)_T > 0 \end{array} . \tag{9}$$

These equations show that ζ and n may simultaneously decrease while leaving $\Delta\mu(\zeta,n)$ constant, as schematized by the transition line "b" in Fig. 2. This line stands for a change in the dynamics and, considering that in the final parts of the transformation the diffusional regime is approached, one may associate the *dynamic* transition to the onset of *configurational* transitions, i.e., to the actual increase of the configurational entropy. One in general expects that $\Delta\mu$ fluctuates along this regression path; however, assuming a constant $\Delta\mu$ suffices for the following arguments [note that this condition is also compatible with the constraint $\overline{\Delta\mu} = \text{const.}$ imposed above for the derivation of $p(\zeta,n)$].

As illustrated above, small-scale relaxation starts when λ is large enough to promote local rearrangements involving the first z units. When the actual threshold energy has reached values ζ^* verifying Eq. (8), these units have the possibility to either follow back the original $n = \text{const.}$ line of a steady rearrangement regime (a in Fig. 2), or take a path in which both n and ζ decrease while keeping $\Delta\mu$ constant (line b in Fig. 2). In other words, a progressive lowering of ζ along path b is associated to a corresponding decrease of the minimum number $\widetilde{\lambda}$ of units, which are necessary to maintain a sufficient dynamic interface to keep following the transition. Since the configurational entropy is independent of n and ζ, Eq. (8) keeps holding throughout and the value $n = 0$ is eventually reached.

Let m be the number of units that have undergone the transition from high to low ζ states at some stage of the regression path. At the beginning of the transition $m = 0$ and $\widetilde{\lambda} = \lambda$, while at the end $\widetilde{\lambda} = 0$; we then consider $\widetilde{\lambda}$ to be a function of m, and the derivative $d\widetilde{\lambda}/dm$ indicates to what extent the minimum number of interfacial units may decrease while still allowing for a further increase of m. This derivative is (on average) negative and we seek a reasonable guess for it, since the cooperativity would be given by $N_\alpha = z[1 + \int_\lambda^0 (dm/dx)\,dx]$. To this aim, one has to consider that the condition $\overline{\Delta\mu} = \text{const.}$ implies that any small-scale rearrangement within a subsystem whatsoever, consisting of, e.g., N units, takes place under the condition that the excess free energy $N\overline{\Delta\mu}$ is a constant. The occurrence of a structural transition must not change this free energy, so the equality $\lambda\Delta\mu(\zeta^*,n) = m_{\max}\Delta\mu(\zeta_{\text{fin}},0)$ holds (ζ_{fin} being the value of the energy threshold at the end of the regression path). Hence, $m_{\max} = \lambda$ and $dm/d\widetilde{\lambda} = -1$, on average. The large-scale cooperativity would thus be given by

$$N_\alpha \approx z(\lambda + 1). \tag{10}$$

Before comparing this expression with the other proposed in Ref. [10] [Eq. (12) below], it may be worth some consideration.

The decrease of energy threshold envisaged in the regression mechanism described above requires that the dynamic interface units deliver energy to the heat bath (which encompasses also the vibrational degrees of freedom) efficiently enough. Indeed, the average energy of these units follows the same evolution of n and ζ. The hypothesis of such an efficient energy exchange underlies also the expression of the average square temperature fluctuations $\overline{\delta T^2}$ central to Donth's theory [2,10]:

$$\overline{\delta T^2} = \frac{k_B T^2}{N_\alpha}\,\Delta\left(\frac{1}{c_p}\right), \tag{11}$$

where $\Delta(1/c_p)$ stands for the change of inverse specific heat across the glass transition temperature T_g. Indeed, the specific heat of the glass encompasses the contributions of both the local vibrations and the configurational degrees of freedom, which are nondiffusive. This means implicitly that the heat exchange between vibrational and nondiffusive degrees of freedom is much faster than between the diffusional and nondiffusional ones. Such slow energy exchanges occur within a subsystem of finite size, the CRR, without inducing any structural change outside. The same picture underlies the

condition $dm/d\widetilde{\lambda} = -1$: the number λ of units that were initially wandering about fixed positions prior to the transition is on average equal to the number of units that will eventually participate to the large-scale rearrangement.

It now remains to show how Eq. (10) compares with the cooperativity derived in Ref. [10], i.e.,

$$N_\alpha \approx z[1 + \zeta^*/Ts_c], \tag{12}$$

where the effective energy barrier ζ^* is defined by

$$\Delta\mu(\zeta^*,n) \equiv \left[\int_{\zeta_0}^{+\infty} d\zeta\ p\right]^{-1} \int_{\zeta_0}^{+\infty} d\zeta\ p\,\Delta\mu, \tag{13}$$

and the configurational entropy at the temperature T is expressed by $s_c \equiv \Delta c_p \ln(T/T_K)$, being T_K the Kauzmann temperature and Δc_p the specific heat step at T_g. (In Ref. [10] a factor $\kappa \equiv [\int_0^\infty d\zeta\ p\,]^{-1} \int_{\zeta_0}^\infty d\zeta\ p$ multiplies ζ^*/Ts_c in order to average over the whole relaxing system; its effect was marginal in the examples of application considered in that paper, and it is omitted here because we are now focusing on a selected rearranging CRR.)

It will be shown below that the cooperativities given by Eqs. (10) and (12) are approximately the same, since the relationship

$$\lambda \approx \frac{\zeta^*}{Ts_c} \tag{14}$$

holds. Equation (14) says that the energy ζ^* lost upon fluctuation regression by each of the units initiating the rearrangement feeds the configurational entropy of λ units, which were in an interfacial dynamic state at the beginning of the transition; the physical origin of this relationship is clarified below. (Before proceeding further, it is important to note that strict equalities in Eqs. (10), (12), and (14) are not necessary, owing to both the approximate character of the theory and the actual impossibility of direct experimental measurements of N_α.)

To arrive at Eq. (14), we consider the contribution $A^* \equiv \int_{\zeta_0}^{+\infty} p\,a^* d\zeta$ to the potential of Eq. (5), from states that may lead to large-scale rearrangements, with

$$a^* \approx w\langle E\rangle_{\zeta_0,n} - k_B T \ln[\Omega\, w^\lambda], \tag{15}$$

w standing for $w(\zeta^*,n)$ and $\Omega \equiv 1/p(\zeta^*,n)$, that is, Ω is the inverse of a typical value of the probability density in the interval $[\,\zeta_0, +\infty\,[$. Just to illustrate the meaning of the entropy contribution in Eq. (15), we assume for the moment that all states are equally likely and consider the dynamic states contributing to A^* as merged into one, in a sort of discretization of the whole ζ space; then, the set of remaining *possible* values the well depth may take (i.e., those for which $\zeta \lesssim \zeta^*$) is discretized too, and $\Omega - 1$ is their number. Close to the glass transition, Ω is very large and $\Omega\, w^\lambda$ is the number of states, which are made *accessible* owing to the presence of λ units in an interfacial dynamic state.

The chemical potential associated to the clusters of units initiating the rearrangements is zA^*. Since the number of these clusters is a nonconserved quantity, the condition $A^* \simeq 0$ holds (the approximate equality is motivated by the basic character of our theory), in analogy with a gas of photons [19]. Then, interpreting the term proportional to $\ln w^\lambda$ in Eq. (15) as a missing energy, i.e., $\lambda\Delta\mu \equiv (1-w)\langle E\rangle_{\zeta_0,n}$, we find

$$\langle E\rangle_{\zeta_0,n} = k_B T \ln\Omega. \tag{16}$$

This is to say that we are considering the "interfacial" neighboring units as virtually dampening the barrier ζ_0 through the term $\lambda\,\Delta\mu$. Equation (16) refers to a conceptually new rearranging unit, which has lost its original individuality because it now encompasses the effects of other units as parts of the dynamic interface allowing mobility overall. Once this new entity has gained an energy $\langle E\rangle_{\zeta_0,n}$, it maintains mobility irrespective of the structural changes that may take place locally, provided no wells of depth $\zeta > \zeta^*$ form nor the initial fluctuation energy regresses. The variety of conditions (i.e., local well depths in our picture) compatible with the energy of the left-hand side of Eq. (16) is accounted for in the entropy $k_B T \ln\Omega$ and the Boltzmann hypothesis is recovered once more.

This description certainly applies to path a in Fig. 2; but also in the case path b is taken, any of the possible $\zeta \leqslant \zeta^*$ barriers may immediately follow in time the initial one (ζ^*) and this lack of information is accounted for in the entropy of Eq. (16). On average, however, moving along the regression path b the mean threshold $\langle\zeta\rangle$ decreases together with the entropy $k_B \ln\Omega$.

We are now in the condition to arrive at Eq. (14). In fact, the average rearranging energy $\langle E\rangle_{\zeta_0,n}$ is comparable with ζ^*, particularly when $T \sim T_g$; on the other hand, adapting to the present context the general case of a fluctuating subsystem (cf. Eq. (8) above and Sect. 20 in Ref. [19]), one finds that $\Delta\mu(\zeta^*,n) \simeq Ts_c$. Thus, the assumption that $\lambda\Delta\mu$ be a missing energy yields

$$\lambda \simeq (1-w)\zeta^*/Ts_c. \tag{17}$$

This is indeed Eq. (14) because $1-w$ is usually $O(1)$, especially in proximity of T_g.

Equation (17), which will be verified to approximately hold in the following analysis, is by no means important because it implies that, at least for nonconfined systems, the cooperativity N_α can be estimated from just the relaxation function without relying upon additional information [note indeed that the left-hand side of Eq. (17) is one of the fitting parameters of the relaxation function, while the quantities on the right hand side require the knowledge of the specific entropy s_c to be calculated]. Moreover, Eq. (17) holds for both polymeric and low molecular weight liquids and suggests that the assumptions of Ref. [10] resumed in Sec. I are more than just a model.

III. EXPERIMENTAL RESULTS

Polystyrene (PS), Poly(vinyl acetate) (PVAc), Acetaminophen (Ac), and Griseofulvin (Gr) were all purchased by Sigma Aldrich; no particular further treatment was done before use. For the sample preparation and the methodology of the measurements, one can refer to the literature, i.e., Refs. [23–26] for PS, PVAc, Ac, and Gr, respectively. Cooperativities will be estimated from calorimetric data obtained under cooling rates of either 0.5 (PVAc) or 1 K/h (PS, Ac, and Gr), with a superposed peak-to-peak temperature modulation

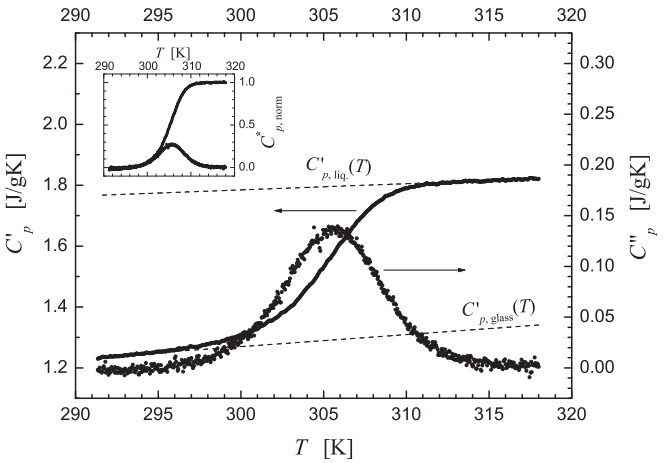

FIG. 3. Real and imaginary parts of the complex heat capacity (in J/gK) of PVAc on cooling, under the experimental conditions illustrated in the main text. $C_{p,\mathrm{liq}}(T)$ and $C_{p,\mathrm{glass}}(T)$ are the equilibrium and unrelaxed heat capacities, respectively. The normalized components of the heat capacity are shown in the inset.

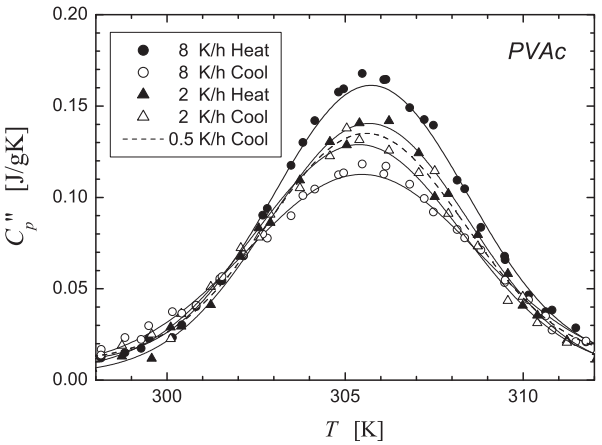

FIG. 4. Imaginary part of the heat capacity C_p'' (in J/gK) for PVAc at different heating/cooling rates. The solid and dashed lines are Gaussian fits (the data points for the cooling rate of 0.5 K/h are not shown for clarity of the figure). The 0.5 K/h heating profile is not reported because it almost completely superposes with the cooling one.

of 1 K at a frequency $\omega = 20.9$ mrad/s, thus selecting a central relaxation time $\tau_0 = 47.8$ s for a symmetric process. As an example, Fig. 3 shows the real and imaginary parts of the complex heat capacity $C_p^* \equiv C_p' - iC_p''$ in PVAc obtained with a cooling rate of 0.5 K/h.

In the following, we chose to carry out our analyses on normalized data:

$$C_{p,\mathrm{norm}}^* \equiv \frac{C_p^* - C_{p,\mathrm{glass}}}{C_{p,\mathrm{liq}} - C_{p,\mathrm{glass}}}, \tag{18}$$

$C_{p,\mathrm{glass}}$ and $C_{p,\mathrm{liq}}$ being the unrelaxed and relaxed heat capacity components, respectively (cf. Fig. 3 in the case of PVAc), extrapolated over the T-domain spanned by the whole relaxation process.

Figure 4 shows the imaginary part of the PVAc heat capacity, C_p'', collected at different scanning rates (cf. Ref. [27] for the corresponding C_p' patterns). On decreasing the latter, the cooling and heating profiles get closer to one another, thus approaching ever more a regime of quasiequilibrium transformation. The dashed line in Fig. 4 refers to a cooling rate of 0.5 K/h and practically coincides with the heating profile (not shown); this indicates that at such a low rate, for a temperature modulation period of 300 s, the system can be considered in equilibrium with good approximation in the temperature region where the peak of the imaginary part of the heat capacity appears.

A. Data analysis

The complex heat capacity C_p^* characterizes the response of a system with respect to (small) temperature changes δT; Ref. [28] provides a simple derivation of a fluctuation-dissipation relation for this quantity, which reads

$$C_p^*(\omega) = -\frac{1}{k_B T^2}\int_0^{+\infty} dt\, e^{-i\,\omega t}\,\frac{\partial \phi_H}{\partial t}, \tag{19}$$

$\phi_H \equiv \langle \Delta H(0)\Delta H(t)\rangle_{\mathrm{eq}}$ being the correlation function of the equilibrium enthalpy fluctuations.

From measurements performed in isothermal conditions (on average) over a sufficiently broad frequency range, $\phi_H(t)$ can be derived by inversion of Eq. (19); the cooperativity then follows by fitting first the result with Eq. (7) and using Eq. (10) afterwards.

On the other hand, in our experimental setup the modulation period is fixed, although a relatively broad temperature interval can be spanned. In order to apply Eq. (7) also in this case, we need to estimate from these data the relevant part of the spectral distribution of $\phi_H(t)$ and associate it with a temperature. This is done by assuming that the time-temperature superposition principle applies [29], i.e., that on changing T the central correlation time of the enthalpy fluctuations rescales by an appropriate shift factor, while the shape of the spectral density remains unchanged. Upon fitting the data using a suitably general analytical expression for ϕ_H, both the distribution of relaxation times and the temperature dependence of the shift factor can be estimated.

Following the customary approaches to the analysis of relaxation data in dielectric or mechanical spectroscopy, ϕ_H will be taken as either a Kohlrausch-Williams-Watts (KWW) stretched exponential, or a function characterized by an Havriliak-Negami (HN) spectral density. One has to be cautious with this kind of assumption; referring for instance to the construction of a master curve via time-temperature superposition from the mechanical response of polycarbonate, O'Connell and McKenna have shown indeed that the stretched exponential may not adequately describe the relaxation features of a system over time domains ranging more than 3–4 decades [30]. In the present case, however, temperature intervals not exceeding 10 K will be explored (see, e.g., Table I) and the spanned range of relaxation times is relatively limited (cf. insets "a" in Fig. 5). Similar conditions were encountered in dielectric studies on PVAc, and indeed a KWW function was found to describe well the relaxation contribution to the response [31].

TABLE I. VFT and shape parameters of the correlation time distributions obtained from data analysis as explained in the text. For PVAc and PS the results were derived from the fittings of Fig. 5 in the indicated T range. For Ac and Gr the results of Refs. [25,26] are reported.

System	T range [K]	$T_{\rm VFT}$ [K]	B [K]	τ_∞ [s]	Shape parameters
PVAc	300.5–310	275.1 ± 0.6	669 ± 28	$(1.3 \pm 0.6) \times 10^{-8}$	$\beta = 0.49 \pm 0.03$
PS	366.5–376	332 ± 0.2	1095 ± 50	$(1.9 \pm 1.3) \times 10^{-10}$	$\begin{cases} a = 0.95 \pm 0.01 \\ b = 0.42 \pm 0.01 \end{cases}$
		$\begin{bmatrix} 334.1_{\rm diel} \\ 341.5_{\rm cal} \end{bmatrix}$ [4]			
Ac[25]	–	240.5	1813	1.1×10^{-13}	$\beta = 0.65$
Gr[26]	–	289.5	2292	5×10^{-14}	$\beta = 0.67$

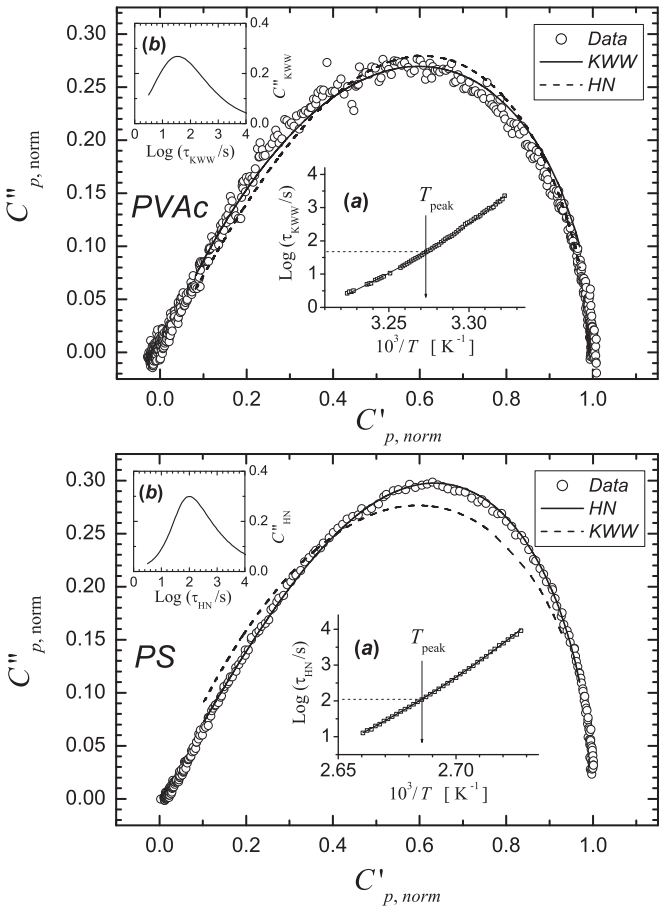

FIG. 5. Cole-Cole representations of $C^*_{p,\rm norm}$ for PVAc (upper panel) and PS (lower panel). The solid lines, which best fit the data, correspond to a KWW relaxation in the case of PVAc and to an HN distribution for PS. The dashed lines represent the lower-quality fits obtained with a HN and a KWW distribution for PVAc and PS, respectively. The $C'_{p,\rm norm}$ intervals in which the analyses have been performed are [0.1,0.97] and [0.08,0.97] for PVAc and PS, respectively. Insets "a" show, each one, the T-dependence of the characteristic relaxation time associated to the solid line of the corresponding main frame (i.e., $\tau_{\rm HN}$ for PS and $\tau_{\rm KWW}$ for PVAc), together with the best VFT approximations. The highlighted temperatures $T_{\rm peak}$ are found by fitting $C''_{p,\rm norm}(T)$ with a Gaussian (cf. the main text and Fig. 6). Insets "b" explicitly report the dependencies of $C''_{\rm HN}$ and $C''_{\rm KWW}$ on τ, after Eqs. (20) and (22), respectively, for the value of ω set by the experimental conditions and the best-fitting shape parameters.

In the case that ϕ_H has an HN spectral density, from Eq. (19) one finds the following expression of the *normalized* heat capacity:

$$C^*_{\rm HN} = \frac{1}{[1 + (i\omega\tau_{\rm HN})^a]^b}, \tag{20}$$

where a and b, both ranging within the]0,1] interval, are the width and asymmetry shape parameters, respectively, and $\tau_{\rm HN}$ is the central relaxation time.

If, on the other hand, the enthalpy correlation is expressed as a stretched exponential, i.e.,

$$\phi_H \equiv \phi_{\rm KWW}(t) = \exp\left\{-\left(\frac{t}{\tau_{\rm KWW}}\right)^\beta\right\}, \tag{21}$$

with β the stretching parameter and $\tau_{\rm KWW}$ a characteristic time, one finds

$$C'_{\rm KWW} = 1 - \omega\tau_{\rm KWW}\int_0^\infty du\, e^{-u^\beta}\, \sin(\omega\tau_{\rm KWW}u)$$
$$C''_{\rm KWW} = \omega\tau_{\rm KWW}\int_0^\infty du\, e^{-u^\beta}\, \cos(\omega\tau_{\rm KWW}u). \tag{22}$$

Of course, $C'_{\rm HN}$ is an invertible function with respect to $\omega\tau_{\rm HN}$ relative to the co-domain]0, 1[, so the function $C''_{\rm HN} \equiv C''_{\rm HN}(C'_{\rm HN})$ can be numerically constructed to fit the data represented in a Cole-Cole plot; the same holds for the KWW case. The fits of both the HN and KWW composite functions to the PVAc and PS data are shown in Fig. 5. The cases of Ac and Gr have been already analyzed along similar lines assuming a stretched exponential decay [25,26] and will not be reconsidered here.

The enthalpy relaxation in PS is described very well by the HN spectral density. In PVAc, fittings of such a quality are not obtained; however, the KWW distribution performs slightly better in this case.

The temperature dependence of the $\tau_{\rm HN}$ relaxation time is obtained from the composite function $[C'_{\rm HN}(\omega\tau_{\rm HN})]^{-1} \circ C'_{p,\rm norm}(T)$, where $C'_{p,\rm norm}(T)$ is defined by the data (cf. the inset of Fig. 3 in the case of PVAc) and the inverse function of $C'_{\rm HN}$ is numerically calculated from Eq. (20) using the best fitting shape parameters. For $\tau_{\rm KWW}(T)$ the procedure is analogous. The insets labeled with "a" in Fig. 5 show these functions. No evident transition from super-Arrhenius to linear dependence at low temperatures, as observed in other studies in proximity of the glass transition temperature [31,32], is perceivable; we recall, however, that the T-range explored here is rather

limited and any such change in T-dependence would hardly be observable (cf., e.g., Fig. 8 in Ref. [31]).

The solid lines in insets "a" of Fig. 5 have been obtained by fitting with the Vogel-Fulcher-Tammann (VFT) expression,

$$\tau = \tau_\infty e^{B/(T-T_{\rm VFT})}, \tag{23}$$

where B is a constant and $T_{\rm VFT}$ is the Vogel temperature. Knowing about the possibility that an Arrhenian dependence might be recovered at low temperatures, we consider Eq. (23) as just a convenient parametrization of the time-temperature dependence: the use of Eq. (23) itself is not presently meant to support, more or less implicitly, any idea about the existence of a hidden phase transition around $T_{\rm VFT}$. This attitude conforms to the spirit of Eq. (10), which, like Donth's Eq. (11), avoids any reference to T_K (or to $T_{\rm VFT}$), in contrast with Eq. (12).

For both the polymer species, all the VFT parameters (i.e., τ_∞, B and $T_{\rm VFT}$) have been left free to adjust; the results are reported in Table I and refer, of course, to the temperature interval in which the analysis has been performed.

In the case of PVAc the fitting procedure yields, as shown in Table I, a Vogel temperature close to that (∼279 K) found for the softening process in recovery compliance measurements [33] (the value $T_{\rm VFT} \simeq 248$ K, characterizing the terminal process in the same mechanical experiment, is similar to that obtained by dielectrics, i.e., $T_{\rm VFT} \simeq 255$ K [8]). With regards to τ_∞, our analysis yields a rather large value ($\sim 10^{-8}$ s). However, if $\tau_\infty \equiv 10^{-14}$ s is imposed (cf. Ref. [34] for a collection of data consistent with this constraint), the resulting Vogel temperature turns out to be very close to that of dielectrics, namely $T_{\rm VFT} = 256.4$ K; the fitting line obtained under this constraint deviates so little from that of Fig. 5, that it is not worth being shown. Of course, one has to keep in mind that, as noticed already, neither of the two forms adopted for the enthalpy correlation function describes the relaxation pattern of Fig. 5 in a completely satisfactory way.

With regards to PS, the HN distribution clearly provides a good description of the process, thus conferring a certain reliability to the fitting results reported in Table I. The Vogel temperature in this case falls in between the values obtained by Plazek for the softening process and the recoverable component of the transition to viscous flow (∼343 and ∼323 K, respectively) in creep compliance measurements [35]. Our result is close to that found from dielectric response, differing by ≈10 K from other calorimetric estimates [4].

As a final step, we associate to the peak temperature of the loss component $C''_{p,\rm norm}(T)$ the relaxation function characterized by the shape parameters worked out in the above analysis (cf. insets "a" and "b" in Fig. 5); this function is then fitted with Eq. (7) and the cooperativity follows after Eq. (10), as stated previously.

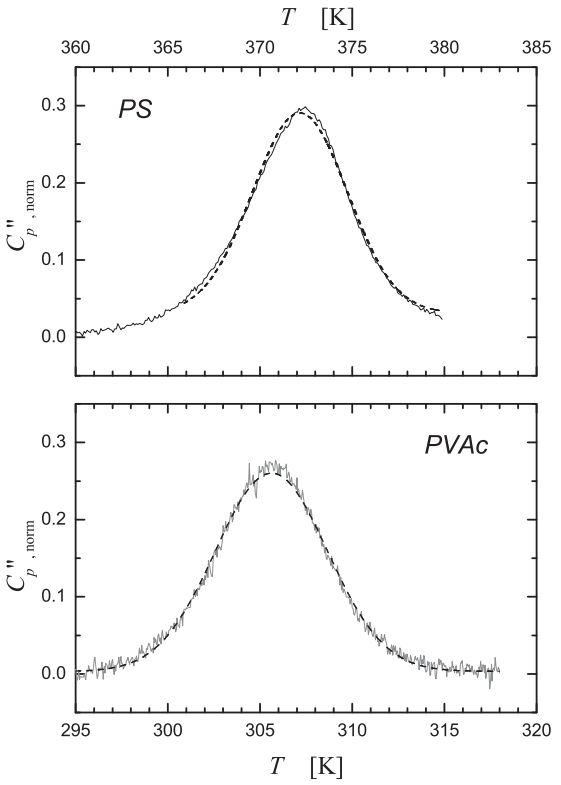

FIG. 6. Imaginary part of the normalized heat capacity of PS (upper panel) and PVAc (lower panel) on cooling. The dashed lines are Gaussian fittings for the estimates of the mean temperature fluctuations.

In the case that Donth's approach is adopted, the $C''_p(T)$ data are simply fitted with a Gaussian [4], i.e.,

$$f \sim e^{-(T-T_{\rm peak})^2/2\delta T^2}, \tag{24}$$

with $T_{\rm peak}$ and δT as adjustable parameters. The resulting values are then used together with $C_{p,\rm liq}(T_{\rm peak})$ and $C_{p,\rm glass}(T_{\rm peak})$ to calculate the cooperativity via Eq. (11). Figure 6 shows the cases of PVAc and PS; for Ac and Gr the same has been done on the data reported in Refs. [25,26].

TABLE II. Peak temperature $T_{\rm peak}$ and half width of the Gaussian δT (K), as obtained by fitting the $C''_{p,\rm norm}(T)$ data with Eq. (24) (for $T_{\rm peak}$ the error is always in the order of 10^{-3} K); equilibrium and unrelaxed (approximate) heat capacities, $C_{p,\rm liq}(T_{\rm peak})$ and $C_{p,\rm glass}(T_{\rm peak})$, respectively, are in J/gK units [for easy reference: molecular weights of 86, 104, 151, and 353 are appropriate for PVAc, PS, Ac, and Gr, respectively, when converting to J/mol · K units] and specific heat step Δc_p in units of k_B at $T_{\rm peak}$. The (approximate) cooperativity N_α, after Eq. (11), is reported in last column.

System	$C_{p,\rm liq}$ [J(gK)$^{-1}$]	$C_{p,\rm glass}$ [J(gK)$^{-1}$]	$\Delta c_p/k_B$	$T_{\rm peak}$ [K]	δT [K]	N_α [Eq. (11)]
PVAc [24]	1.8	1.29	5.21	305.62	2.93 ± .01	240
PS [23]	1.85	1.56	3.75	372.15	2.57 ± .02	170
Ac [25]	1.97	1.31	12	294.35	2.57 ± .03	185
Gr [26]	1.74	1.35	16.8	356.22	2.61 ± .06	75

TABLE III. Fitting parameters (n, λ, z, and $\tau^* \equiv 1/\nu^*$) and relevant outcomes for the thermodynamic variables [$\overline{\Delta\mu}$, $\Delta\mu(\zeta^*,n)$, and ζ^*, all in kJ/mol]. The specific configurational entropy times the temperature, Ts_c (also in kJ/mol), together with the probability $w = \exp\{-\Delta\mu(\zeta^*,n)/k_BT\}$, is used to estimate the ratio $(1-w)\zeta^*/Ts_c$ relating to Eq. (17). The resulting cooperativity N_α as from Eq. (10) is reported in last column.

System	k_BT [$\frac{\text{kJ}}{\text{mol}}$]	Ts_c [$\frac{\text{kJ}}{\text{mol}}$]	n	λ	z	τ^* [s]	$t_{\min}$ [s]	ζ^* [$\frac{\text{kJ}}{\text{mol}}$]	$\overline{\Delta\mu}$ [$\frac{\text{kJ}}{\text{mol}}$]	$\Delta\mu(\zeta^*,n)$ [$\frac{\text{kJ}}{\text{mol}}$]	$(1-w)\zeta^*/Ts_c$	N_α
PVAc	2.51	1.23	43	38.7	5.2	4.5	10	111	1.11	1.89	42.4	205
PS	3.1	1.37	42	31.4	3.6	6.6	20	109	1.25	2.1	47.1	115
Ac	2.13	6.15	43	39.1	3.4	7.5	15	129	1.24	5.87	20.5	135
Gr	3.01	11.3	43	31	3.2	7	5	177	1.58	11.7	15	105

B. Cooperativity estimates

We first derive N_α after Eq. (11); Table II reports the results together with the relevant calorimetric data.

In order to estimate the cooperativities with the relaxation method, we fit the correlation functions within the broadest possible time domains for which $\phi_H \gtrsim 0.1$. Convergence is approached by progressively increasing the exponent n of the density of states until a minimum of the residual variance is achieved [10]. The fitting results are reported in Table III, while Fig. 7 shows some examples.

By comparison with Table II we can see that the two methods provide rather similar values for the cooperativity. On the other hand, the mismatchings between the two sides of Eq. (17) do not exceed a factor of 2, which can be considered acceptable, after the arguments of the theory section. These discrepancies might be mitigated by an improved version of the theory, for instance by allowing a variable number of rearranging units whose average is eventually z. Also a better approximation of A^* could help to resolve this apparent marginal violation of the nonconservation of CRRs number. An improved version of the theory would also allow us to adopt more strict cross-checks of the fitting results. From the latter and the knowledge of Δc_p, for instance, T_K could be derived; however, this requires the inversion of a logarithm in the configurational entropy and error propagation would affect the outcome significantly, so we found this test premature.

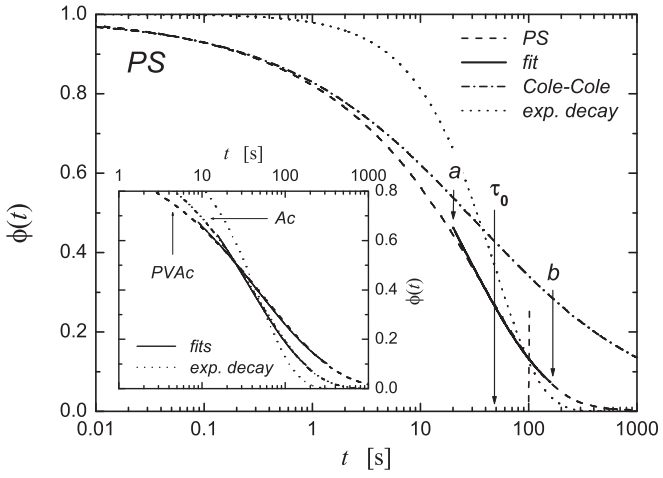

FIG. 7. HN relaxation function (dashed line) and fitting curve (solid line) for PS at $T = 372.2$ K (the shape parameters are reported in Table I). The arrows labeled with "a" and "b" highlight the fitting interval; $\tau_0 \equiv \omega^{-1} \simeq 48$ s is defined by the experimental conditions for a symmetric relaxation. Given ω, the HN shape parameters yield a central relaxation time of ~100 s (highlighted by the vertical dashed line), consistently with inset "b" of the lower panel in Fig. 5. For a comparison, the dotted line refers to a simple exponential decay $\exp\{-t/\tau_0\}$, while the dash-dotted one is the relaxation function of a Cole-Cole process, $[1+(i\,\omega\tau_0)^a]^{-1}$, with $a = 0.46$. The inset compares the PVAc relaxation (dashed) and fitting (solid) at $T = 305.6$ K, with the corresponding ones for Ac (dash-dot-dot and solid, respectively) at $T = 294.3$ K; again the dotted line indicates the single-time exponential decay of the main frame.

IV. INFLUENCE OF THE PROBING METHOD

It has been shown above that once the relaxation function associated to the α process is known, the cooperativity in nonconfined systems, close to the glass transition, can be estimated without resorting to additional information. This raises the question about the possible dependence of these estimates on the spectroscopic method used to extract the distribution of the configurational modes. In other words, we are now concerned with the dependence of the N_α estimates on the parameters characterizing the relaxation function. In the present context we shall limit ourselves to a few examples only.

We start considering the results of an extensive analysis carried out by Colmenero *et al.* [36] on the α-relaxation in poly(vinyl ethylene) (PVE). The frequency- or time-resolved mechanical and dielectric responses of a PVE sample were recorded in isothermal conditions and described by KWW functions associated to the temperatures of the measurements. With respect to the case of the previous section, this way of collecting data has the advantage to avoid the assumption of the time-temperature superposition and to allow following with better resolution the T-dependence of the relaxation function shape parameters.

The stretching exponents in PVE were found to depend on T and to be insensitive (within errors) to the probing technique. However, the characteristic relaxation times observed by mechanical spectroscopy were always about one order of magnitude smaller than those of dielectrics. For a temperature $T = 267$ K, as an example, $\beta_{\text{mech}} \simeq 0.38$ and $\beta_{\text{diel}} \simeq 0.4$, with characteristic times of ~2.5 s and ~50 s, respectively.

We estimated the cooperativity at 267 K assuming a mean $\beta = 0.39$ (deviations of order 0.01 about this value only affect the final result by less than 10% in the present conditions). As shown in Table IV, N_α is almost insensitive to the characteristic

TABLE IV. Results of the relaxation analysis for a sample of PVE at $T = 267$ K. Refer to the caption of Table III for the listed quantities. A $\beta = 0.39$ stretching exponent has been adopted for the relaxation functions in both cases (see main text); for the calculation of the configurational entropy s_c we assumed a Vogel temperature $T_{\rm VFT} = 239.4$ K [36] and a normalized specific heat step at T_g of $\Delta c_p/k_B \simeq 3.38$ [37].

Probing method	k_BT [$\frac{\rm kJ}{\rm mol}$]	Ts_c [$\frac{\rm kJ}{\rm mol}$]	n	λ	z	τ^* [s]	$t_{\rm min}$ [s]	ζ^* [$\frac{\rm kJ}{\rm mol}$]	$\overline{\Delta\mu}$ [$\frac{\rm kJ}{\rm mol}$]	$\Delta\mu(\zeta^*,n)$ [$\frac{\rm kJ}{\rm mol}$]	$(1-w)\zeta^*/Ts_c$	N_α
Diel	2.22	0.82	42	43.9	6.6	2.4	5	92.2	0.89	1.41	53.6	300
Mech	2.22	0.82	43	44.3	7.1	6.9×10^{-2}	0.1	94.7	0.97	1.43	55.6	320

relaxation time and information on the cooperativity seems to be mainly conveyed by the shape (β) of the relaxation function.

This observation finds support when analyzing relaxation functions of different shapes, extracted with different probes from the same system at a given temperature. We chose the α-relaxation in poly(butadiene) (PB) as an example.

On the basis of dielectric measurements, Colmenero *et al.* described the relaxation behavior in this system by means of a stretched exponential with $\beta = 0.41$ or, equivalently, using an HN function with shape parameters $a = 0.72$ and $b = 0.5$ [38,39]. On the other hand, Rössler *et al.* characterized the segmental motion of PB through the reorientational relaxation dynamics observable in ^{2}H-NMR measurements [40]; also in this case a KWW function was used, but the value of the stretching exponent was $\beta = 0.37$. The central relaxation times found with these two methods, though, are similar [9] except for $T \lesssim 180$ K (T_g falls around 170–175 K in the PB samples considered).

More recently, ^{1}H-NMR measurements on PB were analyzed in terms of a rotational diffusion model describing the dynamics of a population of *effective* spin-pairs [9,14]. In this case the distribution of the configurational modes could be described by means of an HN function with shape parameters $a = 0.55$ and $b = 0.45$, corresponding approximately to a stretching exponent $\beta \simeq 0.32$ after Ref. [39]. The VFT curve ($\tau_\infty \equiv 10^{-14}$ s, $B = 1566$ K, and $T_{\rm VFT} = 130$ K) was derived assuming the validity of time-temperature superposition in the interval $193\ {\rm K} \leqslant T \leqslant 273$ K; the central relaxation times obtained by dielectrics remain close to this line down to 174 K.

We consider first the temperature $T = 193$ K (corresponding to a central relaxation time $\tau_0 \sim 10^{-3}$ s) because it is the lowest one at which ^{1}H-NMR data were effectively used to derive both the VFT line and the shape parameters of the HN distribution (cf., e.g., Fig. 2 in Ref. [14]). [As recalled at the end of the previous section, best fitting is approached by steps with increasing n. However, at variance from past analyses (see, e.g., Ref. [10]), after a rapid decrease of the residual variance we found in all cases very slow convergence toward the optimal fitting (in other words, the minimum with respect to n was rather shallow); furthermore, the final cooperativities were too large. For this reason we imposed Eq. (17), i.e., the nonconservation of CRR number, as a prevailing condition with respect to the criterion of minimum variance and stopped increasing n accordingly (of course, reference to s_c cannot be avoided in this situation).] Table V shows that N_α increases with decreasing β.

Approaching T_g more closely, N_α grows. In Table V we compare dielectric and *extrapolated* ^{1}H-NMR results at $T \simeq 174$ K, corresponding to a central relaxation time of $\tau_0 \simeq 30$ s (the case of ^{2}H-NMR is not considered because a value as high as $\sim 10^3$ s was found at this temperature [14,40]). The cooperativities are worked out again as before, i.e., without relying upon Eq. (17) to put a limit to n. Table V still shows that a larger value of N_α is obtained form the analysis of the ^{1}H-NMR relaxation function. This cannot be considered more than an indication, since it is not possible to derive directly the shape parameters and the central relaxation time at so low a temperature by means of the ^{1}H-NMR technique of Ref. [14].

Overall, we find N_α deviations of no more than 30% from the mean, with respect to the different probes considered.

V. CONCLUDING REMARKS

The approach outlined above for the analysis of the α-process in supercooled liquids finds its roots in a statistical mechanical description of energy fluctuations leading to large scale rearrangements. The role of fluctuations, indeed, is central in Donth's theory too; this circumstance possibly motivates, to a large extent, the mutual agreement found in calculating N_α with the two methods.

From the practical point of view, Donth's estimates are based on the direct measurement of the temperature fluc-

TABLE V. Results of the relaxation analysis for PB (data from Refs. [14,38,40]). Refer to the caption of Table III for the listed quantities. In order to estimate s_c, $T_{\rm VFT} = 130$ K (cf. Ref. [14] and references cited therein) and $\Delta c_p/k_B \simeq 3.4$ [41]. The sets of data at the top of the table refer to $T = 193$ K (in which case $Ts_c = 2.15$ kJ/mol), while those in the lower part have been derived at a temperature $T = 174$ K (where $Ts_c = 1.43$ kJ/mol), close to the glass transition of PB (the relaxation function associated to ^{1}H-NMR is an extrapolation at that temperature).

Probing method	τ_0 [s]	n	λ	z	τ^* [s]	$t_{\rm min}$ [s]	ζ^* [$\frac{\rm kJ}{\rm mol}$]	$\overline{\Delta\mu}$ [$\frac{\rm kJ}{\rm mol}$]	$\Delta\mu(\zeta^*,n)$ [$\frac{\rm kJ}{\rm mol}$]	$(1-w)\zeta^*/Ts_c$	N_α
Diel	3.1×10^{-4}	9	8.2	2.5	4.5×10^{-6}	7×10^{-6}	21.2	1.8	3.06	8.4	25
^{2}H-NMR	2.2×10^{-3}	9	8.3	2.9	2×10^{-5}	3×10^{-5}	21.1	1.73	3.04	8.4	30
^{1}H-NMR	6.3×10^{-4}	9	8.2	4.1	6.9×10^{-7}	9×10^{-7}	21.2	1.8	3.06	8.4	40
Diel	30	42	67.6	6.2	1.8	4	65.4	0.57	1.57	30.6	430
^{1}H-NMR	30	35	52.3	9.7	1.8×10^{-2}	5×10^{-2}	42.7	0.73	1.63	26.4	510

tuations accompanying the energy exchanges between the diffusional and nondiffusional degrees of freedom in a CRR; the present method, instead, mainly focuses on the number of units involved in a pre-transitional state, that is, on the dynamic interface.

The concept of a dynamic regime that is intermediate, in a sense, between a condition of frozen configurations and a state where diffusional motion is unconstrained, is fundamental in the present treatment. The establishing of this dynamic state represents at the same time an energy cost to be paid, for a local rearrangement to be possible (this is reminiscent of first order phase transitions), and a means to increase the available number of states in order that appropriate amounts of energy can be attracted from the heat bath.

With regards to the possibility of estimating the cooperativity from just the relaxation function, we may expect the dependence on the probing method as essentially modest. Different experimental techniques, though, provide in general different spectral densities associated with the structural relaxation modes; for this reason one may be induced to consider the cooperativity, i.e., the formation of the dynamic interface, as a common character underlying a variety of observations.

In conclusion, a semiphenomenological approach like the present one has to be considered just a step toward the formulation of a more profound and self-consistent theory. We hope that the issues pointed out so far may be of interest for further advances in this field.

[1] E. Donth, *The Glass Transition: Relaxation Dynamics in Liquids and Disordered Materials*, Springer Series in Materials Science, Vol. 48 (Springer, Berlin, 2001)

[2] E. Donth, J. Polym. Sci. Part B: Polym. Phys. **34**, 2881 (1996).

[3] A. Saiter, L. Delbreilh, H. Couderc, K. Arabeche, A. Schönhals, and J.-M. Saiter, Phys. Rev. E **81**, 041805 (2010).

[4] Y. Z. Chua, G. Schulz, E. Shoifet, H. Huth, R. Zorn Jürn, W. P. Schmelzer, and C. Schick, Colloid Polym. Sci. **292**, 1893 (2014).

[5] C. Dalle-Ferrier, C. Thibierge, C. Alba-Simionesco, L. Berthier, G. Biroli, J.-P. Bouchaud, F. Ladieu, D. L'Hôte, and G. Tarjus, Phys. Rev. E **76**, 041510 (2007).

[6] S. Capaccioli, G. Ruocco, and F. Zamponi, J. Phys. Chem. B **112**, 10652 (2008).

[7] M. Reinecker, V. Soprunyuk, M. Fally, A. Sánchez-Ferrer, and W. Schrantz, Soft Matter **10**, 5729 (2014).

[8] B. Rijal, L. Delbreilh, and A. Saiter, Macromolecules **48**, 8219 (2015).

[9] M. Pieruccini, A. Alessandrini, S. Sturniolo, M. Corti, and A. Rigamonti, Polym. Int. **64**, 1506 (2015).

[10] M. Pieruccini and A. Alessandrini, Phys. Rev. E **91**, 052603 (2015).

[11] M. Pieruccini and T. A. Ezquerra, Eur. Phys. J. E **29**, 163 (2009).

[12] A. S. Keys, J. P. Garrahan, and D. Chandler, Proc. Natl. Acad. Sci. USA **110**, 4482 (2013).

[13] S. Gokhale, K. Hima Nagamanasa, R. Ganapathy, and A. K. Sood, Nat. Commun. **5**, 4685 (2014).

[14] M. Pieruccini, S. Sturniolo, M. Corti, and A. Rigamonti, Eur. Phys. J. B **88**, 283 (2015).

[15] A. Asano, Annu. Rep. NMR Spectrosc. **86**, 1 (2015).

[16] T. Blochowicz, A. Kudlik, S. Benkhof, J. Senker, E. Rössler, and G. Hinze, J. Chem. Phys. **110**, 12011 (1999).

[17] S. Kariyo, A. Brodin, C. Gainaru, A. Herrmann, H. Schick, V. N. Novikov, and E. A. Rössler, Macromolecules **41**, 5313 (2008).

[18] G. Adam and J. H. Gibbs, J. Chem. Phys. **43**, 139 (1965).

[19] L. D. Landau and E. M. Lifšits, *Fisica Statistica*, part I (Editori Riuniti, Roma, 1978).

[20] V. Lubchenko and P. G. Wolynes, J. Chem. Phys. **121**, 2852 (2004).

[21] V. Lubchenko and P. G. Wolynes, Annu. Rev. Phys. Chem. **58**, 235 (2007).

[22] J.-P. Bouchaud and G. Biroli, J. Chem. Phys. **121**, 7347 (2004).

[23] E. Tombari, C. Ferrari, G. Salvetti, and G. P. Johari, Phys. Rev. B **78**, 144203 (2008).

[24] E. Tombari, C. Ferrari, G. Salvetti, and G. P. Johari, Phys. Rev. B **77**, 024304 (2008).

[25] E. Tombari, S. Presto, G. P. Johari, and Ravi M. Shanker, J. Pharm. Sci. **95**, 1006 (2006).

[26] E. Tombari, S. Presto, G. P. Johari, and Ravi M. Shanker, Pharm. Res. **25**, 902 (2007).

[27] E. Tombari, C. Ziparo, G. Salvetti, and G. P. Johari, J. Chem. Phys. **127**, 014905 (2007).

[28] J. K. Nielsen and J. C. Dyre, Phys. Rev. B **54**, 15754 (1996).

[29] G. Strobl, *The Physics of Polymers* (Springer-Verlag, Berlin/Heidelberg, 1996).

[30] P. A. O'Connell and G. B. McKenna, Polym. Eng. Sci. **37**, 1485 (1997).

[31] J. Zhao and G. B. McKenna, J. Chem. Phys. **136**, 154901 (2012).

[32] G. B. McKenna and J. Zhao, J. Non-Cryst. Solids **407**, 3 (2015).

[33] D. J. Plazek, Polymer J. **12**, 43 (1980).

[34] B. Böhmer, K. L. Ngai, C. A. Angell, and D. J. Plazek, J. Chem. Phys. **99**, 4201 (1993).

[35] D. J. Plazek, J. Phys. Chem. **69**, 3480 (1965).

[36] J. Colmenero, A. Alegria, P. G. Santangelo, K. L. Ngai, and C. M. Roland, Macromolecules **27**, 407 (1994).

[37] T. Sakaguchi, N. Taniguchi, O. Urakawa, and K. Adachi, Macromolecules **38**, 422 (2005).

[38] A. Arbe, D. Richter, J. Colmenero, and B. Farago, Phys. Rev. E **54**, 3853 (1996).

[39] F. Alvarez, A. Alegria, and J. Colmenero, Phys. Rev. B **44**, 7306 (1991).

[40] E. Rössler, A. P. Sokolov, P. Eiermann, and U. Warschewske, Physica A **201**, 237 (1993).

[41] M. Bähr, F. Schreier, J. Wosnitza, H. V. Löhneysen, C. Zhu, X. Qin, H. Chen, X. Liu, and X. Wu, Europhys. Lett. **22**, 443 (1993).